

Graviton propagator, renormalization scale and black-hole like states

X. Calmet¹, R. Casadio², A.Yu. Kamenshchik^{2,3}, O.V. Teryaev^{4,5}

¹*Department of Physics & Astronomy, University of Sussex,
Falmer, Brighton, BN1 9QH, United Kingdom.*

²*Dipartimento di Fisica e Astronomia, Università di Bologna, and INFN,
Via Irnerio 46, 40126 Bologna, Italy.*

³*L.D. Landau Institute for Theoretical Physics of the Russian Academy of Sciences,
Kosygin str. 2, 119334 Moscow, Russia.*

⁴*Bogoliubov Laboratory of Theoretical Physics, Joint Institute for Nuclear Research,
141980 Dubna, Russia.*

⁵*Lomonosov Moscow State University,
Leninskie Gory 1, 119991, Moscow, Russia*

Abstract

We study the analytic structure of the resummed graviton propagator, inspired by the possible existence of black hole precursors in its spectrum. We find an infinite number of poles with positive mass, but both positive and negative effective width, and studied their asymptotic behaviour in the infinite sheet Riemann surface. We find that the stability of these precursors depend crucially on the value of the normalisation point scale.

Keywords: gravitons, renormalization, black holes

PACS: 04.60-m, 04.70.D, 11.10.Gh

1. Introduction

Propagators play a crucial role in both quantum mechanics (see e.g. [1]) and in quantum field theory (see e.g. [2, 3]). As is well-known, the appearance of a pole in the free field propagator ($p^2 = m^2$) tells us that there exists a one-particle state with the corresponding mass m . The vacuum polarization loops summation for the photon propagator in quantum electrodynamics revealed the existence of a particular pole at a huge negative value of p^2 [4], which is called the “Landau pole”. Because of gauge invariance, the existence of this pole implies the same pole in the effective charge of the electron. The latter can be removed by imposing causality and using some adequate analytic properties of propagators [5, 6]. The

Email addresses: x.calmet@sussex.ac.uk (X. Calmet¹), Roberto.Casadio@bo.infn.it (R. Casadio²), Alexander.Kamenshchik@bo.infn.it (A.Yu. Kamenshchik^{2,3}), teryaev@theor.jinr.ru (O.V. Teryaev^{4,5})

generalisation of this procedure was later applied to quantum chromodynamics (QCD) [7], resulting in the successful description of various physical processes [8].

More recently, the resummed one-loop propagator of the graviton interacting with matter fields was obtained [9, 10] (see also Appendix A). This propagator has a rather elegant, but involved form, namely

$$i D^{\alpha\beta}(p^2) = i (L^{\alpha\mu} L^{\beta\nu} + L^{\alpha\nu} L^{\beta\mu} - L^{\alpha\beta} L^{\mu\nu}) G(p^2) , \quad (1)$$

where

$$L^{\mu\nu}(p) = \eta^{\mu\nu} - \frac{p^\mu p^\nu}{p^2} \quad (2)$$

and

$$G^{-1}(p^2) = 2p^2 \left[1 - \frac{N p^2}{120 \pi m_{\text{P}}^2} \ln \left(-\frac{p^2}{\mu^2} \right) \right] . \quad (3)$$

Here, m_{P} denotes the Planck mass, μ is the renormalization scale, $N = N_s + 3 N_f + 12 N_V$, where N_s , N_f , N_V are the number of scalar, fermion and vector fields, respectively. In the Standard Model, $N_s = 4$, $N_f = 45$, $N_V = 12$ and $N = 283$. The propagator (1) has a standard pole at $p^2 = 0$ and an infinite number of other poles, which are the zeros of the expression (A.3). It was suggested that these poles correspond to the appearance of a sort of precursors of quantum black holes in Refs. [11, 12].

In this paper we shall study in detail the poles and discuss their possible physical interpretations. In particular, we reveal a multi-sheet structure of the corresponding Riemann surface, the role of the renormalisation point and some analogies with studies of the propagator in QCD.

2. Poles of the graviton propagator

We shall now proceed to study the structure of the graviton propagator that follows from the expression (A.3). We shall in particular derive expressions for the mass and width, and analyse their location in the Riemann surface.

2.1. Pole positions

It is convenient to rewrite the equation for the non-trivial zeros of (A.3) as

$$z \ln z = -A , \quad (4)$$

where the new variable z is defined as

$$z \equiv -\frac{p^2}{\mu^2} \quad (5)$$

and the positive constant

$$A = \frac{120 \pi m_{\text{P}}^2}{N \mu^2} . \quad (6)$$

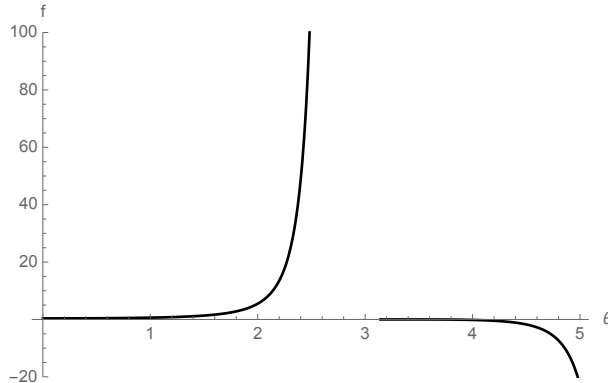


Figure 1: Function f for $0 < \theta < 2\pi$. Solutions of Eq. (12) can only exist in $0 < \theta < \pi$ where $f > 1/e > 0$.

Note that (4) is nothing but the well known Lambert equation [13]. Introducing as usual $z = \rho e^{i\theta}$, we can rewrite (4) as a pair of equations for the imaginary and real parts of the expression on the left-hand side, that is

$$\ln \rho \sin \theta + \theta \cos \theta = 0 , \quad (7)$$

$$\rho \ln \rho \cos \theta - \rho \theta \sin \theta = -A . \quad (8)$$

First of all, let us consider the particular case when $\theta = 0$. Then, Eq. (7) is satisfied automatically, while Eq. (8) takes the form

$$\rho \ln \rho = -A . \quad (9)$$

This equation has two solutions if $A < 1/e$, which merge at $A = 1/e$. Since $z = \text{Re}(z) > 0$, the real part of the corresponding pole for p^2 is negative and both these solutions are tachyons. Obviously, they are stable because $\text{Im}(p^2) = 0$.

If $\theta \neq n\pi$ (with n integer), it follows from Eq. (7) that

$$\ln \rho = -\frac{\theta}{\tan \theta} . \quad (10)$$

Substituting (10) into Eq. (8) yields

$$\rho = \frac{A \sin \theta}{\theta} . \quad (11)$$

Combining Eqs. (11) and (10), we obtain the equation for the phase θ ,

$$f(\theta) \equiv \frac{\theta}{\sin \theta} \exp \left(-\frac{\theta}{\tan \theta} \right) = A , \quad (12)$$

where the function $f(\theta)$ is plotted for $0 < \theta < 2\pi$ in Fig. 1.

Obviously, we are interested only in solutions of Eq. (12) which correspond to a positive ρ from (11). Note, however, that solutions of Eq. (12) exist only if θ and $\sin \theta$ have the

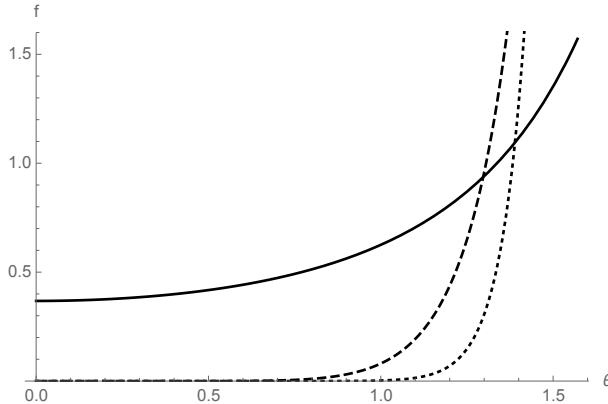


Figure 2: Function f for $n = 0$ with $0 < \theta < \pi/2$ (solid line), for $n = 1$ with $2\pi < \theta < 5\pi/2$ (dashed line) and for $n = 2$ with $4\pi < \theta < 9\pi/2$ (dotted line). Note the origin is shifted to $2n\pi$.

same sign, in which case the right-hand side of Eq. (11) is positive, as required. Therefore, Eq. (12) has solutions only in the intervals

$$2\pi n < \theta < (2n + 1)\pi, \quad n = 0, 1, 2, \dots \quad (13)$$

and in the mirror symmetric intervals with negative values of θ . At the same time, no solutions exist in the intervals

$$(2n + 1)\pi \leq \theta \leq (2n + 2)\pi, \quad n = 0, 1, 2, \dots \quad (14)$$

and in the mirror intervals.

Let us consider the behaviour of the function $f(\theta)$ in Eq. (12) for $0 \leq \theta < \pi$ (the interval (13) with $n = 0$). In this interval, $f(\theta)$ grows monotonically from the minimum $f(0) = 1/e$ to the particular value

$$f\left(\frac{\pi}{2}\right) = \frac{\pi}{2}, \quad (15)$$

where $\rho(\pi/2) = 1$, and then diverges for $\theta \rightarrow \pi$. That means that Eq. (12) has no roots if $A \leq 1/e$ (excluding the two real roots of Eq. (9) already described above), has one root in the interval $0 \leq \theta < \pi/2$ if $1/e \leq A < \pi/2$, and one root in $\pi/2 \leq \theta < \pi$ if $A \geq \pi/2$. It also implies that, for $A > \pi/2$, the equation for the phase has a unique root with $\pi/2 \leq \theta < \pi$, and the corresponding z has a negative real part and a positive imaginary part.

As we are interested in the complete complex structure of the resummed graviton propagator, we shall consider the whole Riemann surface with all of its sheets. On the second sheet, the relevant interval is given by Eq. (13) with $n = 1$, that is $2\pi < \theta < 3\pi$. Here, the function (12) grows from 0 to $5\pi/2$ when the phase θ goes from 2π to $5\pi/2$, and then keeps on growing indefinitely. A comparison of $f(\theta)$ near its minimum at $2\pi n$ for $n = 0, 1$ and 2 is shown in Fig. 2, from which we see that the curve of $f(\theta)$ moves to the right and gets steeper for increasing n (this trend continues for larger values of n). It is worth remarking that this minimum is always $f(2\pi n) = 0$ except for the fundamental sheet $n = 0$, where $f(0) = 1/e$. In general, larger values of A result in larger values of the phases θ_n of the pole positions z_n , and the dependence of the phase θ_n on n will be analysed in more detail below.

2.2. Mass and width

The poles of propagators in the complex domain correspond to unstable particles and this relation is provided by the famous Breit-Wigner formula [14]. This formula may be presented in various ways [15, 16], all of which practically coincide for non-relativistic particles. The covariant representation of the standard non-relativistic formula leads to the parametrization for the pole position given by

$$p^2 = (m - i\Gamma/2)^2 = m^2 - i\Gamma m - \Gamma^2/4 , \quad (16)$$

which is suggested to be the preferable one (see Refs. [15, 16]). We will hence use this expression for the interpretation of the poles of the graviton propagator. We would like to mention also the rather common expression

$$p^2 = m^2 - i\Gamma m , \quad (17)$$

which is obviously close to Eq. (16) for narrow resonances with $\Gamma \ll m$.

Note that the expression (16) is more suitable for investigating wide resonances. In particular, a negative real part of p^2 can be reconciled with positive m^2 , which is not the case for (17). We shall dwell on this point in more detail. Let us try to find the parameters m and Γ corresponding to the poles found in the previous subsection. Comparing the real and imaginary parts of Eq. (16) with those of the position of a pole, we obtain

$$m^2 - \frac{\Gamma^2}{4} = -\mu^2 \rho_n \cos \theta_n , \quad (18)$$

and

$$\Gamma = \frac{\mu^2 \rho_n \sin \theta_n}{m} , \quad (19)$$

where the index n labels the sheet in Eq. (13). On substituting Eq. (19) into Eq. (18), we obtain a quadratic equation for m^2 . The first solution is given by

$$m_1^2 = \mu^2 \rho_n \sin^2 \left(\frac{\theta_n}{2} \right) , \quad (20)$$

$$\Gamma_1^2 = 4\mu^2 \rho_n \cos^2 \left(\frac{\theta_n}{2} \right) ,$$

with m_1^2 and Γ_1^2 positive definite and their ratio

$$\frac{\Gamma}{m} = 2 \cot \left(\frac{\theta_n}{2} \right) . \quad (21)$$

The second solution may also be obtained from the first one by interchanging $m \leftrightarrow 4i\Gamma$ and

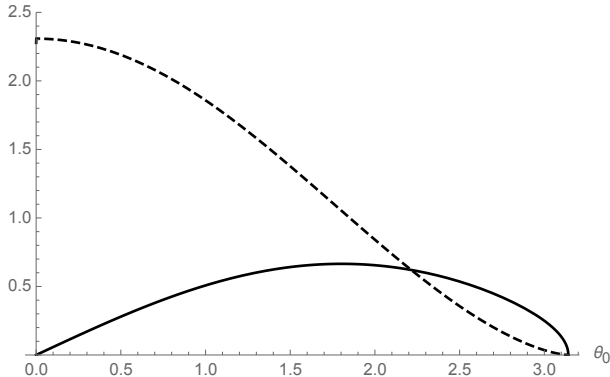


Figure 3: Mass m (solid line) and width Γ (dashed line) in units of m_P versus the pole phase $0 < \theta_0 < \pi$.

reads

$$\begin{aligned}
m_2^2 &= -\mu^2 \rho_n \cos^2\left(\frac{\theta_n}{2}\right), \\
\Gamma_2^2 &= -4\mu^2 \rho_n \sin^2\left(\frac{\theta_n}{2}\right), \\
\frac{\Gamma_2}{m_2} &= -2 \tan\left(\frac{\theta_n}{2}\right),
\end{aligned} \tag{22}$$

with m_2^2 and Γ_2^2 negative definite. Obviously, the second solution (22) implies an imaginary mass m and an imaginary value of Γ . Imaginary m and Γ make the appeal to the Breit-Wigner type of the representation for the poles in the propagator meaningless, and we therefore completely discard Eq. (22) henceforth.

Let us then consider the solution (20) and further require that m is positive, so that the corresponding expression for the width is given by

$$\Gamma = \frac{\mu \sqrt{\rho_n} \sin \theta_n}{|\sin(\theta_n/2)|}. \tag{23}$$

Note that to any positive value of θ_n there corresponds a mirror negative value. Thus, we have pairs of poles with positive mass and both positive and negative values of the width Γ . In principle, it would also be possible to fix Γ positive and similarly get a pair of positive and negative masses. The appearance of such pairs of either Γ or m is simply related to the fact that Eq. (12) is even in θ .

Let us also remark that, had we chosen the representation (17) for the poles of the propagator, we would not be able to avoid the appearance of the negative mass squared and imaginary masses and widths for the poles with $\cos \theta_n > 0$. Thus, the choice of the representation (16) and the solution (20) looks justified in the case of the graviton propagator.

Now, using Eqs. (11) and (6), we can rewrite the expression for the mass as

$$m = m_P \sqrt{\frac{120 \pi}{N} \frac{\sin \theta_n}{\theta_n} \left| \sin\left(\frac{\theta_n}{2}\right) \right|}, \tag{24}$$

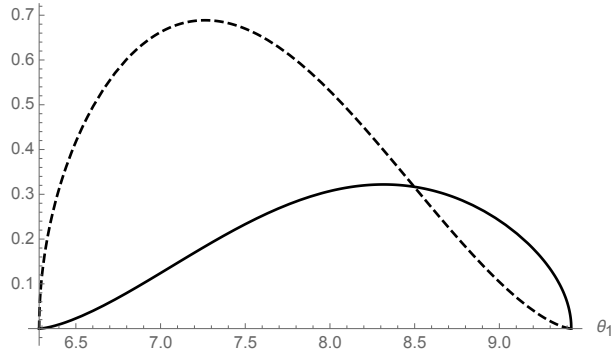


Figure 4: Mass m (solid line) and width Γ (dashed line) in units of m_P versus the pole phase $2\pi < \theta_1 < 3\pi$.

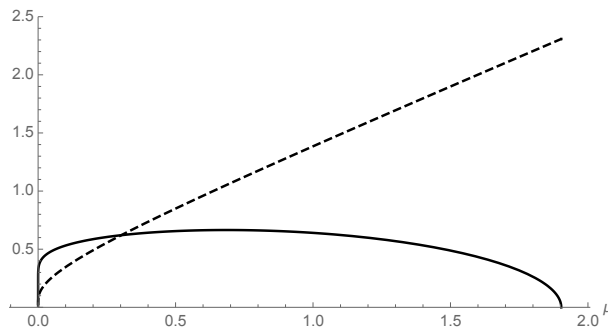


Figure 5: Mass m (solid line) and width Γ (dashed line) versus the renormalisation scale μ (in units of m_P) for a pole in the fundamental sheet $n = 0$.

and the width as

$$\Gamma = m_P \sqrt{\frac{120 \pi \sin \theta_n}{N \theta_n}} \frac{\sin \theta_n}{|\sin(\theta_n/2)|}, \quad (25)$$

and note that their ratio is again simply given by

$$\frac{\Gamma}{m} = 2 \cot\left(\frac{\theta_n}{2}\right), \quad (26)$$

Remarkably, these physical quantities depend only on the total number of fields N and the phase θ_n of the pole, but not on the renormalisation scale μ^2 . We should however not forget that their very existence depends on the value of A which contains μ^2 .

The mass and width are plotted for $0 < \theta_0 < \pi$ in Fig. 3, from which it appears that the Breit-Wigner approximation $\Gamma \ll m$ holds for θ_0 close to π . The specific case considered in Refs. [11, 12] is characterised by $m \simeq \Gamma$ and precisely occurs at $m \approx m_P/2$. The mass and width are also plotted for the next sheet, with $2\pi < \theta_1 < 3\pi$ in Fig. 4, and a similar behaviour appears in higher sheets: the maximum value of the mass m and width Γ decrease with n , and the Breit-Wigner approximation holds for (relatively) large θ_n .

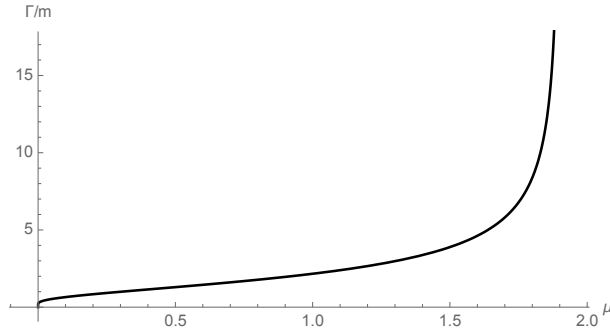


Figure 6: Ratio Γ/m versus the renormalisation scale μ (in units of m_P) for a pole in the fundamental sheet $n = 0$.

2.3. Riemann sheets

It is now interesting to look at the mass m and width Γ as functions of the renormalisation scale μ . This can be done by expressing μ as a function of the phase θ_n from Eq. (12) and then plotting m and Γ parametrically with respect to μ . For the fundamental sheet with $n = 0$, the mass m and the width Γ are shown in Fig 5 and their ratio in Fig. 6. From these graphs, we see again that $m \simeq \Gamma \simeq \mu \simeq m_P$, in agreement with Refs. [11, 12].

For describing the situation in sheets with $n > 0$, we find it convenient to fix the value of the renormalisation scale μ , hence A , and show the dependence of the phase θ_n , mass m and width Γ on n . For $\mu = m_P$, the difference $\Delta_n \equiv \theta_n - 2\pi n$ is plotted in Fig. 7, from which we see that Δ_n starts out smaller than $\pi/2$ and then asymptotes to $\pi/2$ monotonically from below. The corresponding mass m and width Γ are shown to decrease monotonically in Fig. 8, and their ratio (displayed in Fig. 9) asymptotes from above to $\Gamma/m = 2$, in agreement with Eq. (21). For $\mu = m_P/10$, the picture changes slightly. The shift Δ_n is initially larger than $\pi/2$ but decreases below it for increasing n , and eventually asymptotes to $\pi/2$ again from below (see Fig. 10). The mass and width in Fig. 11 behave qualitatively the same as before, but their ratio starts out smaller than $\Gamma/m = 2$, crosses over and then asymptotes to $\Gamma/m = 2$ again from above (see Fig. 12).

These behaviours can in fact be explained analytically from Eq. (12). Let us write $\Delta_n = \delta_n + \pi/2$, so that

$$\theta_n = 2\pi n + \pi/2 + \delta_n \equiv \bar{\theta}_n + \delta_n . \quad (27)$$

For $n \gg 1$, we can then see that $|\delta_n| \ll 1$. In fact, upon replacing (27) into Eq. (12), we obtain

$$\bar{\theta}_n e^{-\bar{\theta}_n \delta_n} \simeq A , \quad (28)$$

to leading order in δ_n , that is

$$\delta_n \simeq \frac{1}{\bar{\theta}_n} \ln\left(\frac{A}{\bar{\theta}_n}\right) . \quad (29)$$

Since $\bar{\theta}_n$ will become necessarily larger than A , for sufficiently large n , the logarithm will become negative and $\delta_n < 0$ will asymptotically vanish. This clearly explains why Δ_n always asymptotes to $\pi/2$ from below. Moreover the ratio Γ/m asymptotes to 2 because of Eq. (21)

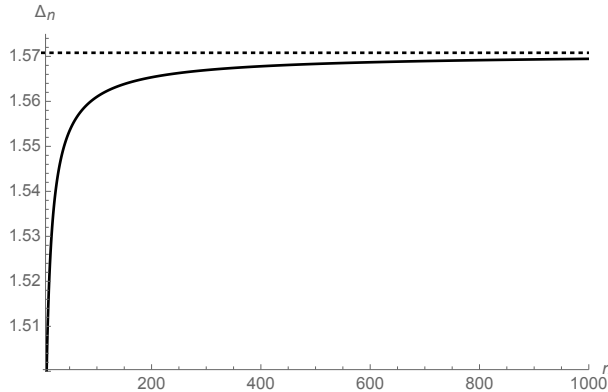


Figure 7: Phase $\Delta_n \equiv \theta_n - 2\pi n$ for $\mu = m_P$ and $n = 1$ to $n = 1000$ (solid line). The dotted line is the asymptote $\pi/2$.

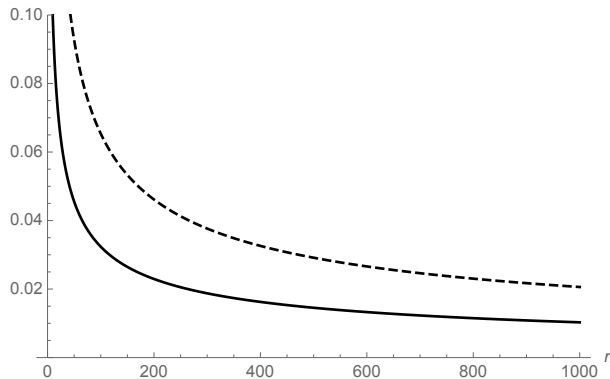


Figure 8: Mass m (solid line) and width Γ (dashed line) for $\mu = m_P$ and $n = 1$ to $n = 1000$.

and does so from above because $\delta_n < 0$ for sufficiently large n . Finally, let us note that for large n we have

$$m \sim \Gamma \sim \frac{1}{\sqrt{\theta_n}} \sim \frac{1}{\sqrt{n}}. \quad (30)$$

3. Physical interpretation

In this paper we have studied the analytic structure of the resummed graviton propagator [9, 10], inspired by the possible existence of black hole precursors [11, 12]. Remarkably, this structure depends essentially on the value of the renormalisation scale parameter μ^2 . It is instructive to compare this situation with the more studied cases of the QED and the QCD. In QED, the choice of the renormalisation point is conveniently performed in the classical limit, when the value of the charge is extracted from macroscopic measurements. At the same time it is possible to trade the dependence on the normalisation point μ^2 in favour of the parameter Λ_{QED} , which is connected with the Landau pole [4], whose value is very large. In QCD, the analogous parameter Λ_{QCD} is typically of hadronic mass scale.

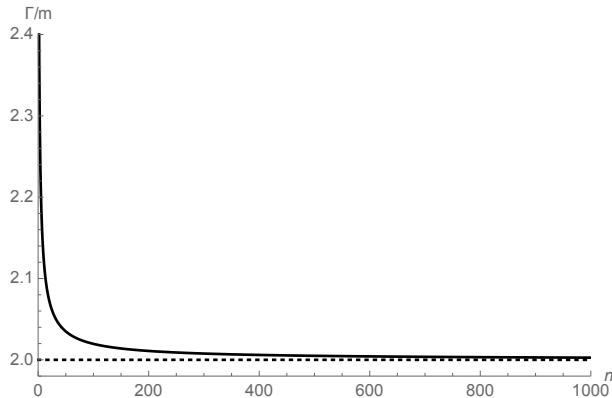


Figure 9: Ratio Γ/m for $\mu = m_{\text{P}}$ and $n = 1$ to $n = 1000$. The asymptote is $\Gamma/m = 2$ (dotted line).

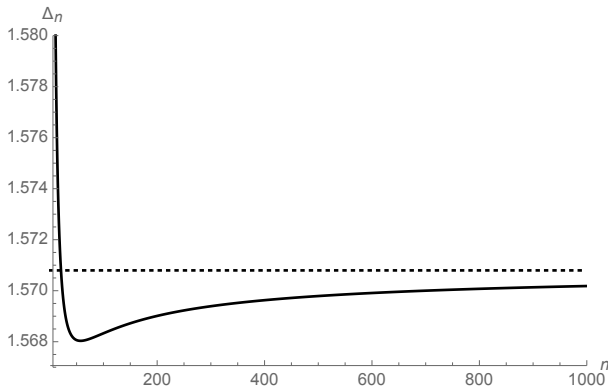


Figure 10: Phase $\Delta_n \equiv \theta_n - 2\pi n$ for $\mu = m_{\text{P}}/10$ and $n = 1$ to $n = 1000$ (solid line). The dotted line is the asymptote $\pi/2$.

Since QCD does not admit a classical limit, this parameter is the one used for describing experimental data [7, 8].

Since gravity is not renormalisable, it must be treated as an effective theory with no parameter equivalent to Λ , and the dependence on the renormalisation scale μ^2 cannot be avoided. In order to have stable black hole-like quasi-particles in the spectrum, one would need widths $\Gamma \ll m$, which our analyses in turn showed would require a renormalisation scale $\mu^2 \ll m_{\text{P}}^2$. In any case, the number of such states would be finite, since the ratio Γ/m grows with the sheet number n towards the asymptotic value $\Gamma/m = 2$. On the other hand, the existence of such quasi-particle states with positive Γ implies the existence of equal mass states with negative Γ . One might speculate these states would be white hole precursors, although this physical interpretation is not completely clear to us. Perhaps highly unstable black and white hole-like states in higher Riemann sheets are not dangerous because of their highly virtual character and the cancellation of the corresponding imaginary parts in the amplitudes involving the graviton propagator. One should mention here that complex conjugated singularities do appear in the Gribov theory of quark confinement [17]. They appear in the solutions of the Schwinger-Dyson equation in QCD [18, 19] and also in the

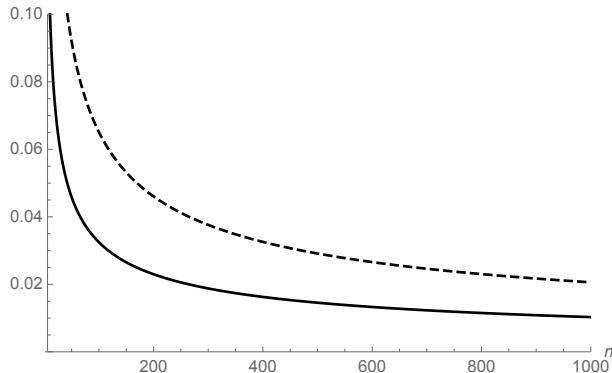


Figure 11: Mass m (solid line) and width Γ (dashed line) for $\mu = m_{\text{P}}/10$ and $n = 1$ to $n = 1000$.

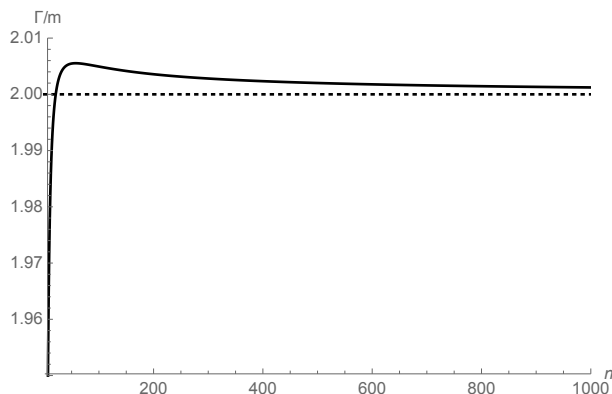


Figure 12: Ratio Γ/m for $\mu = m_{\text{P}}/10$ and $n = 1$ to $n = 1000$. The asymptote is $\Gamma/m = 2$ (dotted line).

extra-dimensional field theories [20].

It is perhaps more compelling to consider the lower Riemann sheets, where poles with positive mass come likewise with both positive and negative width. In order to deal with the states with negative Γ in lower Riemann sheets, one can consider (at least) two options. The first one is to define the contour of integration for computing the propagator in position space in such a way as to exclude these poles, in the spirit of Refs. [5, 6]. In that case, the extra imaginary phase due to the black hole width might lead to observable effects, at least in principle, in particular, to single spin asymmetries [21]. Another option is to assume the renormalisation scale $\mu^2 \gtrsim m_{\text{P}}^2$, so that $|\Gamma| \gtrsim m$ and these states appear only as virtual particles. We conclude by saying that the connection between the black hole type states and the effective quantum field theory deserves further investigation. For instance, non-perturbative effects might come into play at scales of the order of m_{P} , which would require a different analysis like the one in Ref. [12].

Acknowledgments.

We are indebted to D. Kazakov, E. Kolomeitsev, C. Roberts, G. Venturi and R. Yahibbaev for useful discussions. O.T. would like to thank INFN for kind hospitality during October

2016. X.C. is supported in part by the Science and Technology Facilities Council grant N. ST/J000477/1. R.C. and A.K. are partly supported by the INFN grant FLAG. A.K. was partially supported by the RFBR grant N. 17-02-01008. O.T. was partially supported by the RFBR grant N. 17-02-01108.

Appendix A. Gravitational action and propagator

As shown in [22], the resummed propagator (1) can be seen as coming from the variation with respect of the metric field $g_{\mu\nu}$ of the linearized version of the effective action

$$S = \int d^4x \sqrt{-g} \left[\frac{\bar{m}_{\text{P}}^2}{2} \mathcal{R} + c_1 \mathcal{R}^2 + c_2 \mathcal{R}_{\mu\nu} \mathcal{R}^{\mu\nu} + b_1 \mathcal{R} \log\left(\frac{\square}{\mu^2}\right) \mathcal{R} + b_2 \mathcal{R}_{\mu\nu} \log\left(\frac{\square}{\mu^2}\right) \mathcal{R}^{\mu\nu} + b_3 \mathcal{R}_{\mu\nu\rho\sigma} \log\left(\frac{\square}{\mu^2}\right) \mathcal{R}^{\mu\nu\rho\sigma} \right], \quad (\text{A.1})$$

where \mathcal{R} , $\mathcal{R}^{\mu\nu}$ and $\mathcal{R}^{\mu\nu\rho\sigma}$ are respectively the Ricci scalar, Ricci tensor and Riemann tensor and \bar{m}_{P} is the reduced Planck mass. The Wilson coefficients c_1 and c_2 are arbitrary within the effective field theory approach, and should be fixed by comparing with experimental data. On the other hand b_1 , b_2 and b_3 are calculable from first principles and related to N .

The resulting complete propagator for the graviton then contains the function

$$G^{-1}(p^2) = 2p^2 \left[1 - 16\pi c_2 \frac{p^2}{m_{\text{P}}^2} - \frac{N p^2}{120\pi m_{\text{P}}^2} \ln\left(-\frac{p^2}{\mu^2}\right) \right]. \quad (\text{A.2})$$

Clearly the position of the poles of (A.2) will depend on the value of c_2 , which is arbitrary. For the self-healing mechanism to work, $c_2 = c_2(\mu)$ should be suppressed by $1/N$ in comparison to the coefficients b_i [23]. Let us also stress that Eq. (A.2) can be formally rewritten in the same form as Eq. (1), namely

$$G^{-1}(p^2) = 2p^2 \left[1 - \frac{N p^2}{120\pi m_{\text{P}}^2} \ln\left(-e^{1920\pi^2 c_2} \frac{p^2}{\mu^2}\right) \right], \quad (\text{A.3})$$

so that the analytic structure does not change and our analysis still applies.

References

- [1] B.R. Holstein, *Topics in Advanced Quantum Mechanics*, (Dover, New York, 2014).
- [2] N.N. Bogoliubov, D.V. Shirkov, *Introduction to the theory of quantized fields*, (John Wiley, New York, 1980).
- [3] V.B. Berestetskii, E.M. Lifshitz and L.P. Pitaevskii, *Quantum Electrodynamics: Volume 4*, (Elsevier Science, Amsterdam, 1982).
- [4] L.D. Landau, A.A. Abrikosov and I.M. Khalatnikov, Dokl. Akad. Nauk SSSR 95 (1954) 773; Dokl. Akad. Nauk SSSR 95 (1954) 1177; Dokl. Akad. Nauk SSSR 96 (1954) 261.

- [5] P.J. Redmond, Phys. Rev. **112** (1958) 1404.
- [6] N.N. Bogolyubov, A.A. Logunov and D.V. Shirkov, Sov. Phys. JETP **37** (1960) 574.
- [7] D.V. Shirkov and I.L. Solovtsov, Phys. Rev. Lett. **79** (1997) 1209; Theor. Math. Phys. **150** (2007) 132.
- [8] A.P. Bakulev, S.V. Mikhailov and N.G. Stefanis, Phys. Rev. D **72** (2005) 074014; M. Baldicchi, A.V. Nesterenko, G.M. Prospero, D.V. Shirkov and C. Simolo, Phys. Rev. Lett. **99** (2007) 242001; R.S. Pasechnik, D.V. Shirkov and O.V. Teryaev, Phys. Rev. D **78** (2008) 071902 A.P. Bakulev, S.V. Mikhailov and N.G. Stefanis, JHEP **1006** (2010) 085; V.L. Khandramai, R.S. Pasechnik, D.V. Shirkov, O.P. Solovtsova and O.V. Teryaev, Phys. Lett. B **706** (2012) 340.
- [9] T. Han and S. Willenbrock, Phys. Lett. B **616** (2005) 215.
- [10] U. Aydemir, M.M. Anber and J.F. Donoghue, Phys. Rev. D **86** (2012) 014025.
- [11] X. Calmet, Mod. Phys. Lett. A **29** (2014) 1450204.
- [12] X. Calmet and R. Casadio, Eur. Phys. J. C **75** (2015) 445.
- [13] R.M. Corless, G.H. Gonnet, D.E.G. Hare, D.J. Jeffrey and D.E. Knuth, Adv. Comput. Math. **5** (1996) 329.
- [14] G. Breit and E. Wigner, Phys. Rev. **49** (1936) 519.
- [15] T. Bhattacharya and S. Willenbrock, Phys. Rev. D **47** (1993) 4022.
- [16] A.R. Bohm and Y. Sato, Phys. Rev. D **71**, 085018 (2005).
- [17] V.N. Gribov, in Nyiri, J. (ed.), *The Gribov theory of quark confinement*, 162-184 [hep-ph/9403218]; in Nyiri, J. (ed.), *The Gribov theory of quark confinement*, 185-191 [hep-ph/9404332]; in Nyiri, J. (ed.), *The Gribov theory of quark confinement*, 192-203 [hep-ph/9905285]; Eur. Phys. J. C **10** (1999) 91.
- [18] G. Krein, C.D. Roberts and A.G. Williams, Int. J. Mod. Phys. A **7** (1992) 5607; C.J. Burden, C.D. Roberts and A.G. Williams, Phys. Lett. B **285** (1992) 347.
- [19] P. Maris, Phys. Rev. D **52** (1995) 6087
- [20] D.I. Kazakov and G.S. Vartanov, JHEP **0706** (2007) 081.
- [21] O.V. Teryaev, R.M. Yahibbaev, work in progress.
- [22] X. Calmet, S. Capozziello and D. Pryer, in preparation.
- [23] E. Tomboulis, Phys. Lett. **70B** (1977) 361.